Investigation of polymer electrolyte membrane fuel cell internal behaviour during long term operation and its use in prognostics

Lei Mao [a, *], Lisa Jackson [a], Tom Jackson [b]

[a] Department of Aeronautical and Automotive Engineering, Loughborough University, Leicestershire, LE11 3TU, UK
[b] Centre for Information Management, Loughborough University, Leicestershire, LE11 3TU, UK

HIGHLIGHTS

- PEM fuel cell internal behaviour during the lifetime is investigated.
- PEM fuel cell future performance is predicted using internal behaviour evolution.
- Multiple particle filters are used to predict PEM fuel cell performance.
- Prognostic analysis can give reliable prediction especially at dynamic condition.

ABSTRACT

This paper investigates the polymer electrolyte membrane (PEM) fuel cell internal behaviour variation at different operating condition, with characterization test data taken at predefined inspection times, and uses the determined internal behaviour evolution to predict the future PEM fuel cell performance. For this purpose, a PEM fuel cell behaviour model is used, which can be related to various fuel cell losses. By matching the model to the collected polarization curves from the PEM fuel cell system, the variation of fuel cell internal behaviour can be obtained through the determined model parameters. From the results, the source of PEM fuel cell degradation during its lifetime at different conditions can be better understood. Moreover, with determined fuel cell internal behaviour, the future fuel cell performance can be obtained by predicting the future model parameters. By comparing with prognostic results using adaptive neuro fuzzy inference system (ANFIS), the proposed prognostic analysis can provide better predictions for PEM fuel cell performance at dynamic condition, and with the understanding of variation in PEM fuel cell internal behaviour, mitigation strategies can be designed to extend the fuel cell performance.

© 2017 The Author(s). Published by Elsevier B.V. This is an open access article under the CC BY license (http://creativecommons.org/licenses/by/4.0/).

1. Introduction

In the last few decades, many efforts have been devoted to the innovative energy generation sources to reduce the emissions. Among these sources, hydrogen and fuel cells, especially the polymer electrolyte membrane (PEM) fuel cells, have received much attention, since they are the zero emission energy conversion and power generation devices. As the results, PEM fuel cells have already been equipped in real applications including stationary power station, automotive and consumer devices.

However, the reliability and durability of PEM fuel cells are still two major barriers for the further commercialization, where many practical fuel cell systems, especially those at dynamic loading conditions like in automotive application, cannot reach the designed requirement of useful life. As a possible solution, a series of research has been devoted to the fault detection and isolation of fuel cells in the last few decades [1—12], which can be used to evaluate the operating status of fuel cell system, thus mitigation strategies can be carried to recover the fuel cell performance in case of fuel cell faults. The techniques involved in these studies can be loosely divided into two groups, including model-based and data-driven approaches. Regarding the model-based methodologies, the model representing fuel cell behaviour should be developed, by comparing the residuals between model outputs and actual measurements, fuel cell faults can be detected, and the faults can also be isolated by minimizing the residuals with updated model

---

* Corresponding author.
  E-mail address: l.mao@lboro.ac.uk (L. Mao).

parameters [1–6]. While in the data-driven approaches, the measurements from fuel cell system will be analyzed, features indicating fuel cell performance are extracted, and the system state can be determined by applying pattern recognition algorithms to the extracted features [7–12].

Compared to the fuel cell fault diagnostic studies, only few researches have been performed to predict the fuel cell future performance and determine its remaining useful life (RUL) [13–22]. Due to the difficulty of developing an accurate fuel cell model incorporating complete failure mode effects, most studies in fuel cell prognostics are based on black-box models. The general idea in black-box model based prognostics is to derive input-output relationship of the fuel cell system with the training process, and then predict the future fuel cell performance based on the trained model. However, one drawback of these prognostic techniques is that the prognostic performance relies heavily on the quality and quantity of training data, i.e. if the PEM fuel cell system experiences faults in the operation, the trained model cannot provide reliable predictions before re-training the model with the new dataset including the fault information. Moreover, prognostic results from the black-box models cannot provide the understanding of PEM fuel cell internal behaviour, thus it is difficult to design maintenance strategies to extend the PEM fuel cell lifetime based on the prognostic results. On this basis, it is necessary to study the variation of the PEM fuel cell internal behaviour during its lifetime, and predict the future PEM fuel cell performance using the evolution of fuel cell internal behaviour.

In this paper, the internal behaviour of PEM fuel cell system during its lifetime is studied using the PEM fuel cell behaviour model, which can be related to various PEM fuel cell losses. By matching the model parameters to the collected polarization curves with certain interval, the variation of fuel cell internal behaviour can be obtained, which can be used to analyse the source for the PEM fuel cell degradation at both steady state and dynamic conditions. Moreover, with the determined model parameter evolution, the future model parameters are predicted using particle filtering approach, and the future PEM fuel cell performance can then be determined. Furthermore, the prognostic results are compared with those using ANFIS at both steady state and dynamic conditions, results demonstrate that the proposed prognostic analysis can provide better predictions at PEM fuel cell dynamic condition.

2. Description of PEM fuel cell durability tests

The durability tests of PEM fuel cell system described in Ref. [29] are used in this analysis, which includes PEM fuel cell performance at different conditions, including both the steady state and dynamic conditions.

The test bench with electrical power up to 1 kW is used to test the PEM fuel cell performance during its lifetime. In order to control the fuel cell operating conditions more accurately, several parameters related to PEM fuel cells are measured and controlled, which are listed in Table 1, while Table 2 lists the control parameters used in the steady state condition.

The PEM fuel cell stack used in the durability tests contains 5 cells with open cathode, and each cell has active area of 100 cm^2. It should be mentioned that the PEM fuel cell is comprised of a commercial Nafion membrane, platinum nanoparticle catalyst, carbon diffusion materials, silicone sealing gaskets, composite flow field plates having channels for water coolant circuit. The main characteristics of theMEA are listed in Table 3.

The nominal current density of the PEM fuel cell is 0.70A/cm^2 (determined based on the PEM fuel cell output power and its lifetime), and maximum current density is 1 A/cm^2. Fig. 1(a) depicts

Table 1
Range of PEM fuel cell parameters during the test [29].

PEM fuel cell parameter	Range
Cooling temperature (°C)	20–80
Cooling flow (l/min)	0–10
Gas temperature (°C)	20–80
Gas humidification (%)	0–100
Air flow (l/min)	0–100
Hydrogen flow (l/min)	0–30
Gas pressure (bar)	0–2
Fuel cell current (A)	0–300

Table 2
PEM fuel cell parameters in the steady state condition test [29].

PEM fuel cell parameter	Value
Fuel cell current (A)	70
Anode inlet temperature (°C)	28
Cathode inlet temperature(°C)	42
Anode inlet flow rate (l/min)	4.8
Cathode inlet flow rate (l/min)	23
Cooling flow (l/min)	2
Gas inlet hygrometry (%)	50
Anode inlet pressure (mbar)	1300
Cathode inlet pressure (mbar)	1300

Table 3
PEM fuel cell characteristics.

| Parameter	Value
Membrane thickness	25 μm
Active area	100 cm × 100 cm
Platinum loading	0.2 mg/cm^2
Gas diffusion thickness	415 μm
Flow channel	7-fold serpentine

the schematic diagram of the PEM fuel cell test and current densities for different conditions, while Fig. 1(b) shows the current densities applied to the PEM fuel cell stack at steady state and dynamic conditions, respectively.

It can be seen from Fig. 1(b) that the 1st test studies the durability of the fuel cell stack in steady state regime, where the PEM fuel cell stack is operated at nominal current density. While the fuel cell stack durability under dynamic condition is tested in the 2nd test, and current density with high-frequency current ripples is applied to simulate the dynamic condition. The reason of using 0.7 A/cm^2 with high-frequency current ripples is to let the dynamic current density comparable to the nominal current density used in the 1st durability test, thus the results from these tests can provide the clear understanding about the performance variation at different operating conditions.

3. Investigation of PEM fuel cell internal behaviour

In the above described PEM fuel cell durability tests, the polarization curve test is carried out once a week (with about 160 h interval), and the collected polarization curves at the two durability tests are depicted in Fig. 2. It should be noted that the mean fuel cell voltage is used in this analysis, so that the internal behaviour within single cell can be investigated instead of the fuel cell stack. Moreover, for better illustration purpose, only some polarization curves are depicted in Fig. 2 to better demonstrate the PEM fuel cell performance change during the tests.
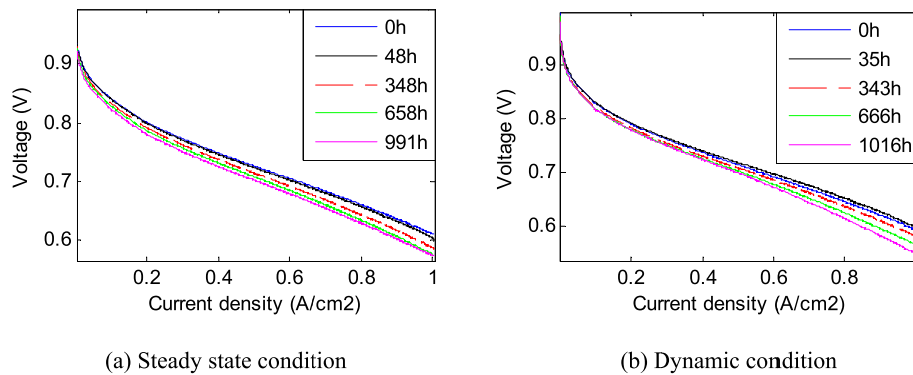
It can be found from Fig. 2 that during the long term operations (about 1000 h herein), the PEM fuel cell performance will decay
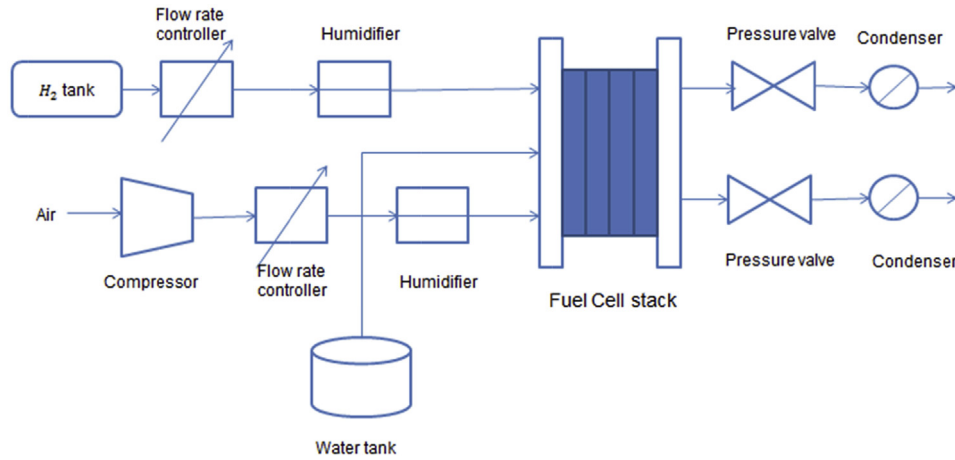
(a)   Schematic diagram of PEM fuel cell durability test

1st durability test   2nd durability test
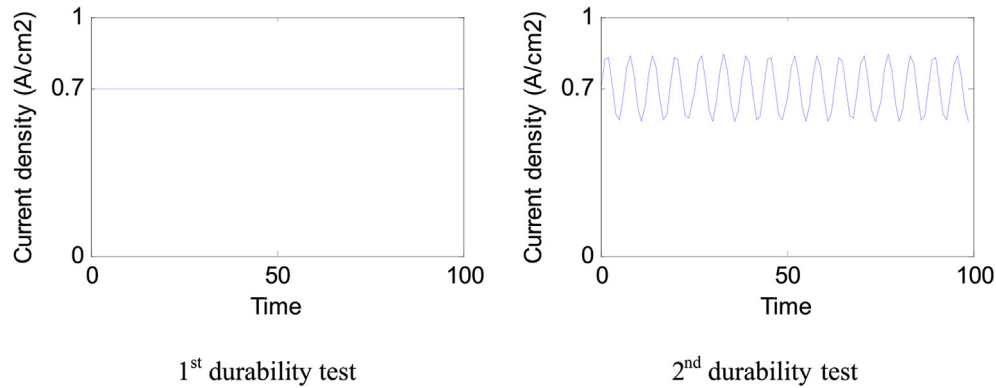
(b) Current densities used in the durability tests [29]

Fig. 1. PEM fuel cell durability test.

(a) Steady state condition   (b) Dynamic condition

Fig. 2. Collected polarization curves during the tests at two different conditions.

over time at both operating condition. However, the fuel cell shows different performance degradation phenomenon at two operating conditions, i.e. at steady state condition, the performance degradation rate will increase at the early operation stage (from 48 h to 658 h in Fig. 2(a)), and then decrease at the end of the fuel cell lifetime, while the PEM fuel cell performance degradation is still clear at the end of its lifetime at dynamic current density condition (shown in Fig. 2(b) from 666 h to 1016 h).

In order to study the evolution of PEM fuel cell internal behaviour during its lifetime, a PEM fuel cell behaviour model is used in this study, which is expressed with the following equation. The reason of using the model is that it can represent several PEM fuel cell losses during the operation, including activation loss, ohmic loss, mass transport loss and fuel crossover loss [24–26], thus the variation of internal fuel cell behaviour can be investigated by studying the changes of model parameters.

$$V = E_{rev} - \frac{RT}{2 \propto F} \ln\left(\frac{i}{i_{oc}}\right) - \frac{RT}{2 \propto F} \ln\left(\frac{i_n}{i_{oc}}\right) - m_{trans} e^{n_{trans} \times i} - i \times R_{mem}$$

(1)

where E_{rev} is reversible cell voltage (1.22 V is used in this study), R is universal gas constant, T is cell temperature, $\propto$ is charge transfer coefficient, with value within the range of 0 and 1 (0.5 in this study), F is faraday constant, i_{oc} is exchange current density at cathode, i_n is internal current density, m_{trans} and n_{trans} are mass transport loss coefficients, R_{mem} is membrane resistance. It should be noted that as the anode activation overvoltage is negligible in comparison to the cathode overvoltage, it is ignored in the above equation. It should be mentioned that the reason of using $m_{trans} e^{n_{trans} \times i}$ to express PEM fuel cell mass transport loss is because it has been used in the previous work for PEM fuel cell modelling, and results show that the PEM fuel cell mass transport loss part can be simulated accurately with the above expression [17].

The variation of model parameters (i_n, i_{oc}, m_{trans}, n_{trans}, and R_{mem}) can be obtained by matching Eq. (1) to the results from characterization tests of PEM fuel cell system, in this study the polarization curve is selected for this purpose. The reason is that polarization curve can express fuel cell losses directly, with different phases in polarization curve corresponding fuel cell loss terms in Eq. (1) [27,28]. Moreover, the polarization curves can be collected easily from the fuel cell system without extra testing equipment, which can reduce the complexity and cost of the monitoring process. Furthermore, with the collection of polarization curve, the fuel cell performance can be recovered effectively, and this recovery effect becomes prominent with the fuel cell operation, this is consistent with the fuel cell aging phenomenon, which will be further studied below.

Fig. 3 depicts the fuel cell stack response from these two durability tests, where the fuel cell stack performance degradation during its lifetime can be clearly observed. It should be noted that in the durability test, characterization tests are carried out once per week, where polarization curves are collected. As mentioned before, the collection of the polarization curve can effectively recover the fuel cell performance, which can be found in Fig. 2 with circled parts in the fuel cell voltage curve, which are consistent with the time when the polarization curve is collected. The possible reason for the performance recovery due to collection of polarization curve is that since different current densities are used, excess water inside the fuel cells can be better removed, thus better water management can be obtained through the collection of polarization curve, and performance degradation due to poor water management can be recovered. In order to make reliable predictions, this recovery effect should be included in the prognostic analysis as it can affect the future fuel cell performance and its RUL, this will be further discussed in the following section.

Moreover, with the voltage evolution obtained from the tests, the voltage degradation rates can be obtained as 0.025 mV/h and 0.03 mV/h at steady state condition and dynamic condition, respectively, indicating that the dynamic loading condition can accelerate the fuel cell degradation. It is noted that as no fuel cell fault is observed during the tests, the degradation rate herein represents the fuel cell aging phenomenon.

With the method described before, the fuel cell model parameters can be obtained by matching Eq. (1) to the collected polarization curve, and results are listed in Tables 4 and 5.

Several observations can be made from the above results. Model parameters show a monotonous trend during the PEM fuel cell durability tests. Compared to the parameter values from 1st durability test, model parameters at 2nd durability test have larger values, especially for i_n and i_{oc}, indicating that the dynamic current density can affect the capability of membrane for preventing ions. Moreover, since the PEM fuel cell system requires a certain time to reach stabilization at the beginning of the test, the model parameters at the starting point (0 h in above tables) may not represent the actual fuel cell performance, thus they are not included in the following analysis.

Fig. 4 depicts the evolutions of model parameters in Eq. (1) at different loading conditions by removing their values at the starting point. To provide a better comparison, the model parameters shown in Tables 4 and 5 are normalized, so that the evolution trend of model parameters can be compared at different fuel cell operating conditions.

It can be seen from above figure that fuel cell model parameters follow a similar evolution trend at different operating conditions, which paves the way of using the same state equation to represent the model parameter evolutions for PEM fuel cell prognostics. However, it can be seen that the dynamic operating condition can cause faster and more dynamic PEM fuel cell degradation, as model parameters will have larger variations at dynamic operating conditions.

Furthermore, the effectiveness of model parameters from curve fitting techniques is studied by comparing the polarization curves collected from the test and simulated using model parameters. Fig. 5 depicts the comparison of polarization curves at two operating conditions. To better illustrate the comparison results, only two polarization curves are shown herein at each operating condition. Moreover, root mean square error (RMSE) is calculated to better evaluate the performance of developed model, which can be calculated using Eq. (2)
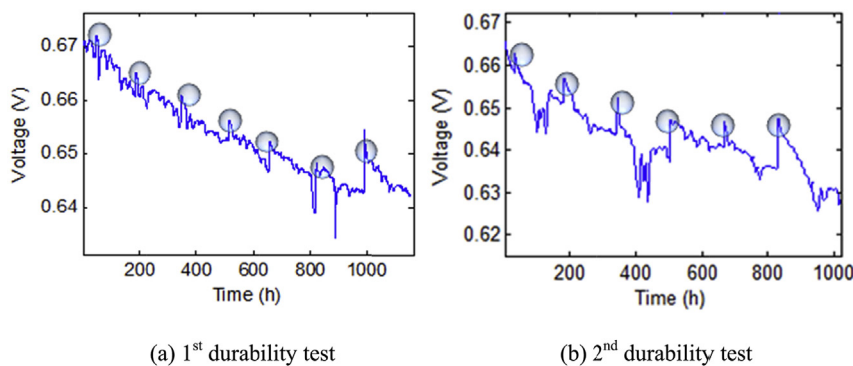

(a) 1st durability test　　　　　　　　(b) 2nd durability test

Fig. 3. Fuel cell stack voltage evolutions at durability tests.

Table 4
Determined model parameters from the 1st durability test.

Model parameter	Operation time (h)							
	0	48	185	348	515	628	823	991
i_n (A/cm^2)	0.00821	0.00493	0.00526	0.00627	0.00751	0.00791	0.00775	0.00775
i_{oc} (A/cm^2)	0.00025	0.00072	0.00047	0.00037	0.00035	0.00021	0.00023	0.00022
m_{trans}	0.3153	0.3454	0.3055	0.3042	0.2456	0.2381	0.2123	0.2345
n_{trans}	0.00767	0.206	0.2845	0.2919	0.3657	0.4024	0.4169	0.3588
R_{mem} (ohm/cm^2)	0.1867	0.09694	0.09848	0.101	0.103	0.09926	0.106	0.112

Table 5
Determined model parameters from the 2nd durability test.

Model parameter	Operation time (h)							
	0	35	182	343	515	666	830	1016
i_n (A/cm^2)	0.00953	0.00767	0.00837	0.00857	0.00949	0.00934	0.00919	0.00946
i_{oc} (A/cm^2)	0.00048	0.00085	0.00081	0.0011	0.00085	0.00066	0.00078	0.00066
m_{trans}	0.1765	0.2658	0.2458	0.225	0.2135	0.1991	0.213	0.2036
n_{trans}	0.4924	0.4187	0.4687	0.4107	0.5843	0.596	0.622	0.645
R_{mem} (ohm/cm^2)	0.089	0.08008	0.08364	0.08564	0.09544	0.09374	0.09717	0.09842

$$RMSE = \sqrt{\frac{\sum_{i=1}^{n}(y_i - \widehat{y}_i)^2}{n}} \qquad (2)$$

where y_t is the actual measurement at time t, and $\widehat{y}_t$ is the output from the model at time t, n is the number of measurement samples. It can be seen that the smaller RMSE indicates better prediction accuracy from the neural networks. Tables 6 and 7 lists the RMSE of the polarization curves collected at different times under steady state and dynamic conditions, respectively. It can be seen that the determined model parameters from curve fitting technique can represent the PEM fuel cell behaviour at two different operating conditions with good quality.

It should be noted that the membrane resistance determined in Tables 4 and 5 are comparable to previous studies [18,19] indicating that the ohmic resistance ranges from 0.009ohm/cm^2 to 0.182ohm/cm^2, which further validate the effectiveness of PEM fuel cell model parameters extracted from the polarization curves.

Moreover, the overvoltage due to different PEM fuel cell losses are calculated and depicted in Fig. 6. It should be mentioned that since i_{oc} is considered as a constant value herein, the overvoltage due to activation loss is also a constant value.

It can be found from the above figure that in the PEM fuel cell durability tests at steady state condition, the mass transport loss accounts for 61% of PEM fuel cell performance degradation, and activation loss accounts for 24% of PEM fuel cell performance degradation, 12% PEM fuel cell degradation results from ohmic loss, only 3% from fuel crossover loss, this is also consistent with the results from previous study [20]. While at dynamic condition, most PEM fuel cell performance degradation is still from mass transport loss (53% in this case), 27% from activation loss, but fuel crossover loss increases clearly at dynamic condition, which makes similar contribution as ohmic loss in this case for the PEM fuel cell performance degradation (10%), indicating that the dynamic condition will reduce the PEM fuel cell capability of preventing gas reactants from pass through the membrane.

4. Use of model parameter evolution for PEM fuel cell prognostics

4.1. Description of particle filtering based prognostic technique

From above section, the evolution of model parameters can be obtained, and PEM fuel cell internal behaviour variation during the lifetime can be determined, which can be used to analyse the source of the fuel cell performance degradation and design effective mitigation strategies. In this section, the future variation of model parameters will be predicted to provide the PEM fuel cell future performance.

In this study, particle filtering approach is used to predict the future model parameters based on the previous evolutions, as this technique has been applied successfully for fuel cell prognostics in previous studies [21—23].

Particle filtering approach is an effective tool for the Bayesian tracking problem of a non-linear system with non-Gaussian noise, which can be defined with the following equations:

$$x_k = f(x_{k-1}, \vartheta_k, v_k) \qquad (3)$$

$$y_k = g(x_k, \mu_k) \qquad (4)$$

where Eq. (3) represents the system state, and Eq. (4) is the observations from the system, ϑ_k are parameters of the system state model, v_k and μ_k are statistically independent identically distributed noise from the system state model and observations, respectively.

The probability density function $p(x_k|y_{1:k})$ is calculated in order to obtain the distribution of possible state x at time k. In the analysis, the initial state distribution $p(x_0)$ should be known, and two stages will be repeated to determine the optimal Bayesian solution, which can be written as:

$$p(x_k|y_{1:k-1}) = \int p(x_k|x_{k-1})p(x_{k-1}|y_{k-1})dx_{k-1} \qquad (5)$$

$$p(x_k|y_{1:k}) = \frac{p(y_k|x_k)p(x_k|y_{1:k})}{p(y_k|x_{1:k-1})} \qquad (6)$$

Theoretically, the optimal solution can be calculated using the above equations, but in most cases the analytical solution cannot be obtained. To address this issue, an approximation can be obtained with the particle filtering approach using the following steps.

Step 1: generate n particles based on the initial system state distribution;

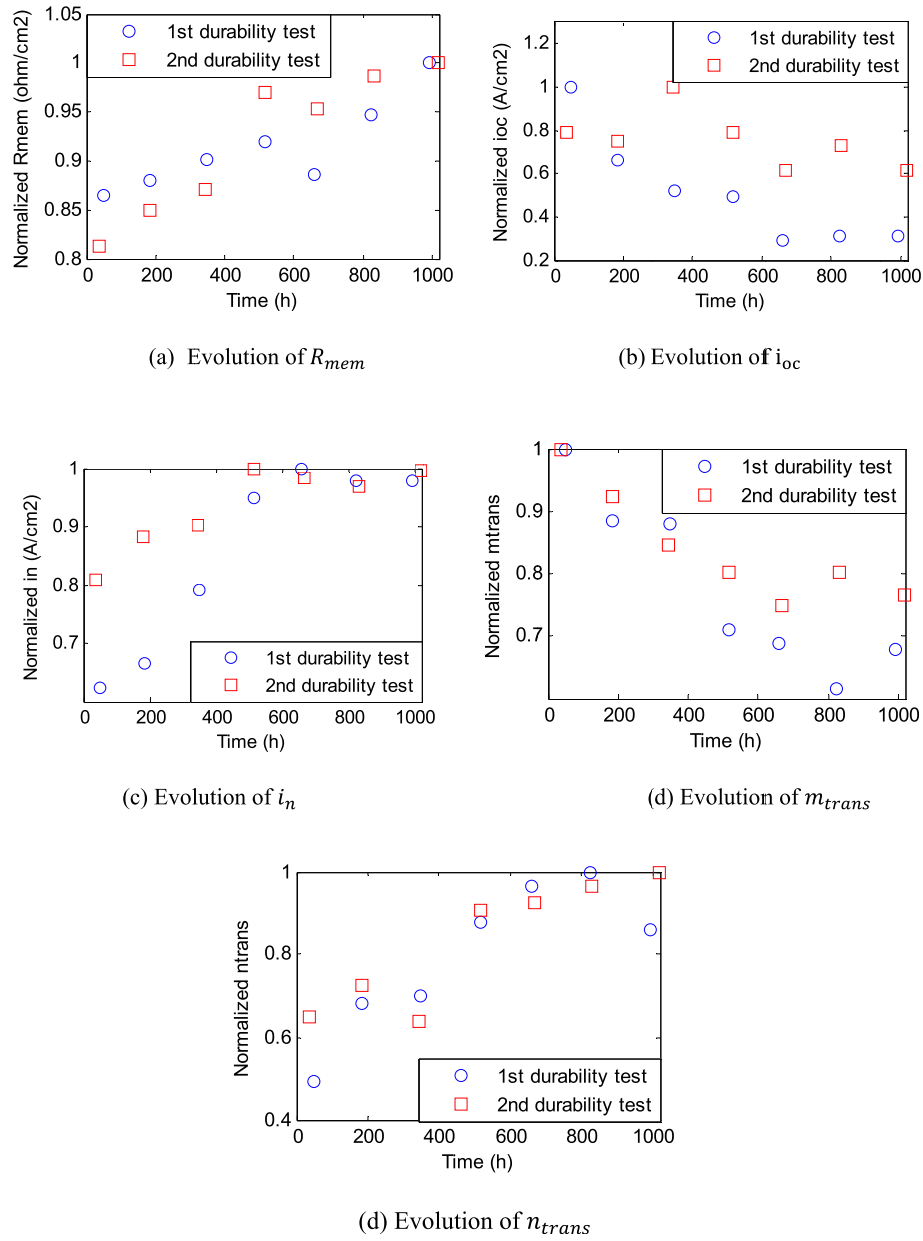*Step 2:* particle will move to the next state (from k-1 to k) using

(a) Evolution of R_{mem}

(b) Evolution of i_{oc}

(c) Evolution of i_n

(d) Evolution of m_{trans}

(d) Evolution of n_{trans}

Fig. 4. Evolution of fuel cell behaviour model parameters during the fuel cell durability tests.

(a) Comparison at 1st durability test
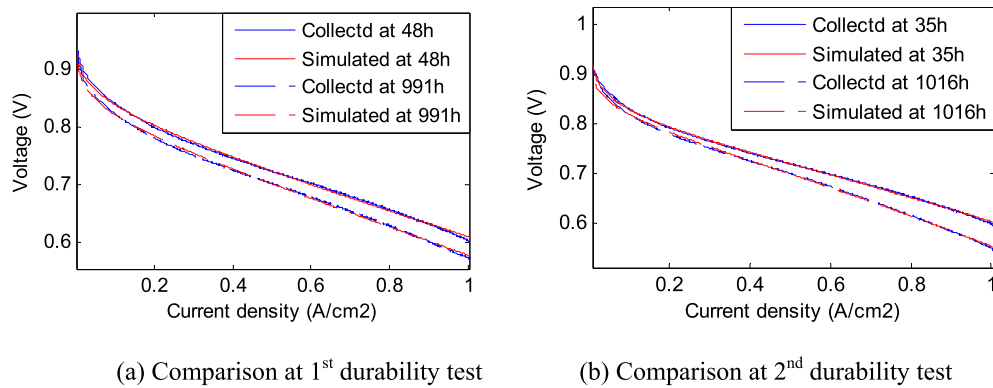
(b) Comparison at 2nd durability test

Fig. 5. Comparison of polarization curves collected from 2 durability tests and simulated using model parameters.

Table 6
RMSE of simulated polarization curve under steady state conditions.

	RMSE						
Time (h)	48	185	348	515	658	823	991
RMSE	2.7×10^{-6}	2.7×10^{-6}	2.5×10^{-6}	2.8×10^{-6}	2.7×10^{-6}	2.6×10^{-6}	2.6×10^{-6}

Table 7
RMSE of simulated polarization curve under dynamic conditions.

	RMSE						
Time (h)	35	182	343	515	666	830	1016
RMSE	3.1×10^{-6}	2.9×10^{-6}	3.0×10^{-6}	3.1×10^{-6}	3.0×10^{-6}	2.8×10^{-6}	3.0×10^{-6}

the state model in Eq. (3);

Step 3: with new observation at time k, the likelihood function $p(y_k|x_k)$ can be calculated, and particle weights can be calculated using the following equation:

$$w_k^{(i)} = \frac{1}{\sqrt{2\pi R}} e^{-\frac{\left(z_k - z_k^{(i)}\right)^2}{2R}} \tag{7}$$

where $w_k^{(i)}$ is the value of ith weight at time step k, R is the variance of measurement error, z_k is the actual measurement at time step k, $z_k^{(i)}$ is the prediction from the ith particle at time step k.

Step 4: re-sample the particles by eliminating particles with lower weights, and duplicating particles with higher weights;

Step 5: repeat steps 2—4 to predict the system state continuously;

It should be noted that as the fuel cell behaviour model shown in Eq. (1) contains multiple parameters corresponding to various fuel cell losses, multiple state equations should be used to reflect the evolution of these parameters, which requires multiple particle filters in the prognostic analysis. With predicted model parameters from multiple particle filters, the fuel cell voltage can be calculated using Eq. (1).

4.2. Determination of state equations for fuel cell model parameters

As described before, state equations are required in the particle filtering approach to predict the future performance of the system, which should be capable of representing the evolution of fuel cell model parameters.

In this study, the curve fitting technique is used to generate the state equations for the fuel cell behaviour model parameters based on the determined evolution of model parameters. The criteria of generated state equations is that these state equations should have a simple format and can represent the model parameter evolution accurately, which can be evaluated using R squared and RMSE values. From the results, the following equations are proposed as the state equations, and coefficient values from two durability tests are listed in Table 8.

Evolution of i_{oc}: $i_{oc}(t) = a_1 - a_2 t \tag{8}$

Evolution of i_n: $i_n(t) = b_1 + b_2 t \tag{9}$

Evolution of R_{mem}: $R_{mem}(t) = c_1 + c_2 t \tag{10}$

Evolution of m_{trans}: $m_{trans}(t) = d_1 e^{d_2 t} \tag{11}$

Evolution of n_{trans}: $n_{trans}(t) = e_1 e^{e_2 t} \tag{12}$

Where a_1, b_1 and c_1 are the initial values for i_{oc}, i_n and R_{mem}, respectively, a_2, b_2 and c_2 represents the PEM fuel cell degradation rate due to activation loss, fuel crossover loss, and Ohmic loss, d_1 and e_1 controls the amplitude of mass transport loss, while d_2 and e_2 express the PEM fuel cell degradation rate due to mass transport loss during the operation.

It can be seen from above table that at dynamic condition, the membrane resistance will be increase more rapidly (indicated with higher c_1 value), and higher internal current density (higher b1 listed in Table 5) indicates dynamic current density will cause loss of membrane capability of preventing iron from passing through. This can better explain the faster degradation and shorted fuel cell lifetime at dynamic conditions.

Moreover, as collection of polarization curve can recover the PEM fuel cell performance effectively, which is depicted in Fig. 2, this effect should be considered when performing fuel cell prognostics. In this study, an equation is proposed using curve fitting technique to represent the performance recovery effect due to polarization curve collection, which is written as the equation below and constant to the previous study [22]. Equation co-efficients at different fuel cell conditions are listed in Table 9.

$$V_{recover}(t) = ae^{bt} + ce^{dt} \tag{13}$$

It can be seen that with the fitted equations, the evolution of recovered fuel cell voltage can provide a high quality simulation. With the fuel cell operation, the recovery effect due to characterization tests is gradually reduced, but at the end of the fuel cell system lifetime, better recovery effect can be observed. Moreover, at the dynamic condition, less recovery effect is observed than that under the steady state condition, this effect, together with faster degraded fuel cell parameters (shown in Fig. 3), leads to the reduced useful life of the fuel cell system under dynamic conditions.

4.3. Prognostic performance using multiple particle filter based technique

From section 2, the fuel cell behaviour model in Eq. (1) contains 5 model parameters with nearly monotonous trend in the durability tests, thus a total of 5 particle filters are used in the analysis to predict each parameter separately. In order to apply particle filters in the analysis, Eqs. (8)–(12) are re-organized in recursive format, which are written below.

Evolution of i_{oc}: $i_{oc}(t+1) = a_2 + i_{oc}(t) \tag{14}$

Evolution of i_n: $i_n(t+1) = b_2 + i_n(t) \tag{15}$

Table 8
Coefficient values of model parameter evolution equations from two durability tests.

Durability test	a_1 (A/cm^2)	a_2 ($A/cm^2.h$)	b_1 (A/cm^2)	b_2 ($A/cm^2.h$)	c_1 (ohm/cm^2)	c_2 ($ohm/cm^2.h$)
1	0.0061	4.79×10^{-6}	0.0050	3.41×10^{-6}	1.34×10^{-5}	0.0956
Durability test	d_1	d_2	e_1	e_2		
1	0.3447	−0.0005	0.237	0.0002		
Durability test	a_1 (A/cm^2)	a_2 ($A/cm^2.h$)	b_1 (A/cm^2)	b_2 ($A/cm^2.h$)	c_1 (ohm/cm^2)	c_2 ($ohm/cm^2.h$)
2	0.0009	2.27×10^{-7}	0.0080	1.69×10^{-6}	1.97×10^{-5}	0.0805
Durability test	d_1	d_2	e_1	e_2		
2	0.2572	−0.0003	0.4153	0.0005		

Table 9
Coefficients in the Eq. (11) for the recovered fuel cell voltage.

	A	b	c	d
Test 1	705	0.00705	0.6738	-6.023×10^{-5}
Test 2	3.89×10^{-5}	0.00669	0.6614	-4.497×10^{-4}

Evolution of R_{mem}: $R_{mem}(t+1) = c_2 + R_{mem}(t)$　　　(16)

Evolution of m_{trans}: $m_{trans}(t+1)$
$$= d_1 e^{d_2 t} \times \left(e^{d_2} - 1\right) + m_{trans}(t)$$ 　　(17)

Evolution of n_{trans}: $n_{trans}(t+1) = e_1 e^{e_2 t} \times (e^{e_2} - 1) + n_{trans}(t)$ (18)

It should be mentioned that the noise is not included in the state equations, since these equations are proposed by matching the collected polarization curves, which already include the measurement noise effect.

As described in section 3.1, new observations (model parameters herein) should be added in the particle filtering approach to calculate the particle weights, but in the analysis, the model parameters are extracted from the polarization curve, which is collected with 1 week interval, thus in the analysis, the time step in Eqs. (14)–(18) is set to be consistent with the time when the polarization curve is collected.

One issue associated with the above time step setting is that the fuel cell voltage cannot be predicted continuously. In order to make the particle filtering approach more suitable in practical applications, the fuel cell degradation rate is added to the particle filtering approach to provide the fuel cell voltage prediction between two consecutive polarization curves. The fuel cell degradation rate can be determined using the following equation.

$$\frac{dV}{dt} = -\frac{RT}{2 \propto F} \frac{dln\left(\frac{i}{i_{oc}}\right)}{dt} - \frac{RT}{2 \propto F} \frac{dln\left(\frac{i_n}{i_{oc}}\right)}{dt} - \frac{dm_{trans}}{dt} e^{n_{trans} \times i}$$
$$- m_{trans} e^{n_{trans} \times i} \frac{dn_{trans}}{dt} \times i - i \times \frac{dR_{mem}}{dt}$$ (19)

where $\frac{dln\left(\frac{i}{i_{oc}}\right)}{dt}$, $\frac{dln\left(\frac{i_n}{i_{oc}}\right)}{dt}$, $\frac{dm_{trans}}{dt}$, $\frac{dn_{trans}}{dt}$ and $\frac{dR_{mem}}{dt}$ in Eq. (19) are calculated using fitted equations in Eqs. (8)–(12).

Following the steps described in section 3.1, multiple particle filters are used in parallel to estimate the model parameters in Eqs. (14)–(18), Table 10 lists the set-up of the particle filters.

Fig. 7 depicts the performance of multi-particle filter based fuel cell prognostic approach in both steady state and dynamic loading conditions. It can be seen that with the multiple particle filter-based prognostic technique, actual fuel cell voltage at constant and dynamic load current conditions can be included using the predicted range (upper and lower bound predictions in Fig. 7), and the predicted fuel cell voltage can effectively capture the actual fuel cell performance.

4.4. Comparison with prognostic results using ANFIS

In order to further study the effectiveness of PEM fuel cell prognostics using predicted model parameters, it is compared with the prognostic results using ANFIS, which has been widely used in fuel cell prognostics [14–17].

A typical ANFIS can include five layers. Layer 1 is the fuzzification layer which performs fuzzification to the incoming inputs. For example, two inputs (x_1, x_2) and 4 membership functions $(P_{11}, P_{21}, P_{12}, P_{22})$ are applied in Fig. 1, then 16 rules (2^4) can be formulated (if-then rule), and the output from layer 1 can be written as in Equation (20).

$$y_i^1 = \mu_{A_i^j}\left(x_i^1\right) = \frac{1}{1 + \left|\frac{x_i^1 - c_i}{a_i}\right|^{2b_i}}$$ (20)

where $\mu_{A_i^j}$ is the fuzzy rule associated with ith input and jth fuzzy rule, y_i^1 is the ith output at layer 1, a_i, b_i and c_i are the parameters in the membership function, which will be adjusted during the training phase.

In layer 2, the firing strength of the fuzzy rule will be generated, with output y_i^2 from layer 2, which is described in Equation (21)

$$y_i^2 = \omega_i = \prod_i \mu_{A_i^j}\left(x_i^1\right)$$ (21)

where ω_i is the firing strength of the rule.

Layer 3 is usually defined as the normalization layer, where the neurons at this layer receive inputs from all neuros at layer 2 and calculate the normalized firing strength, which can be expressed as y_i^3 in Equation (22)

$$y_i^3 = \overline{\omega_i} = \omega_i \Bigg/ \sum_1^i \omega_i$$ (22)

Layer 4 is called the defuzzification layer, each neuro at this layer receives outputs from layer 3 as well as the original inputs of the system (x_1, x_2) for the calculation, with output y_i^4 calculated by Equation (23)

$$y_i^4 = \overline{\omega_i} f_i = \overline{\omega_i}\left(c_1^j x_1 + c_2^j x_2 + c_3^j\right)$$ (23)

where c_1^j, c_2^j and c_3^j are consequent parameters of the jth fuzzy rule, which will be updated during the training process.

With outputs from layer 4, the system output can be calculated with Equation (24)

47

Table 10
Set-up of particle filters.

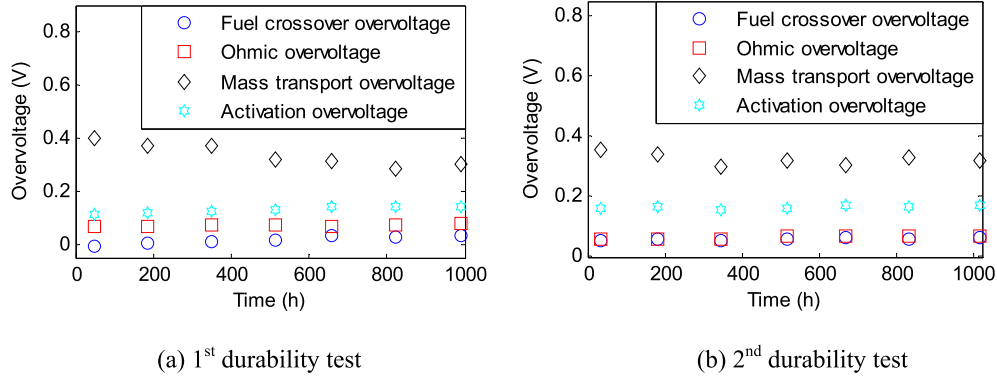| Particle number	500
Initial state	Uniform distribution cantered on the initial parameter value with a range of ± 1% percentage around the value
Re-sampling method	Sequential importance resampling

(a) 1st durability test   (b) 2nd durability test

Fig. 6. Overvoltage due to different PEM fuel cell losses in durability tests.

(a) 1st durability test   (b) 2nd durability test
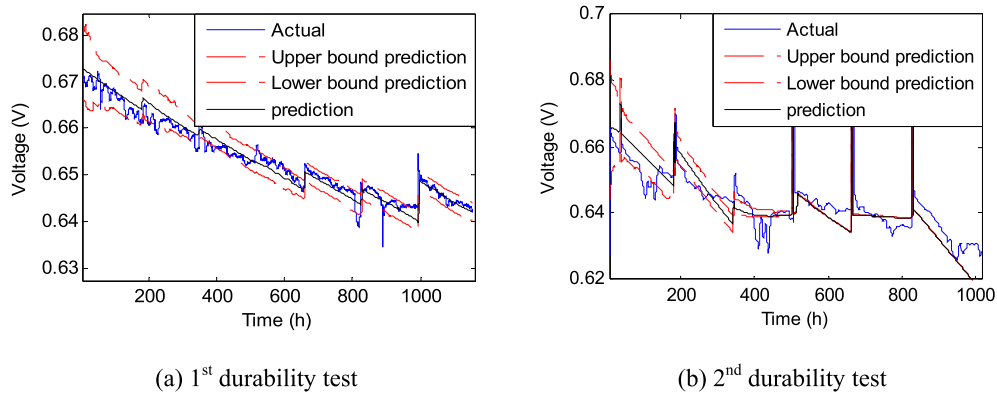
Fig. 7. Prediction results from particle filtering approach for two durability tests.

$$y_i^5 = \sum_i \overline{\omega_i} f_i \qquad (24)$$

It should be noted that the input layer of ANFIS contains 3 inputs, which are the three selected sensor measurements using sensitivity analysis technique proposed in Ref. [17], while the output is the fuel cell voltage. In this study, a single output Sugeno-type fuzzy inference system is used. With a trial and error method, the membership functions for input and output are selected as generalized bell function and linear function, respectively, while the training algorithm uses mixed least squares and backpropagation.

In the study, the test data is divided into two parts, the first 2/3rd of the stack voltages is used to train the ANFIS model, while the last 1/3rd of the test data is employed to validate the performance of the trained ANFIS. Fig. 8 depicts the prediction results at steady state and dynamic loading conditions.

It can be found from Fig. 7(a) and (c) that at steady state condition, the ANFIS can give the reliable fuel cell voltage predictions after the training process, except the two voltage valleys at around 800 h and 900 h, the reason is that these voltage drops are due to the stop of fuel cell system in the test, where the fuel cell system operating condition is changed. This indicates that ANFIS may not

learn and predict the reasonable fuel cell performance under operating condition variation, this can be better illustrated in the prediction results at dynamic loading condition depicted in Fig. 7(b) and (d), misleading fuel cell voltage will appear after 400 h, this is due to the lack of capability of ANFIS in learning and predicting the fuel cell behaviour with varying current.

Furthermore, the prognostic performance using multiple particle filtering approach and ANFIS is compared in terms of computational time and prediction accuracy, where the prediction accuracy is determined using the average value between the prediction and the actual value, the results are listed in Table 11. It can be found that compared to ANFIS, multiple particle filtering approach can provide better prediction at dynamic condition, since it can capture the evolution of fuel cell parameters during the system operation effectively. However, it should be mentioned that as less computation time is used, ANFIS can be selected for PEM fuel cell prognostics in the steady state regime, as fuel cell performance will decay monotonously and can be learned effectively using ANFIS.

5. Conclusion

In this paper, the variation of PEM fuel cell internal behaviour

(a) Prediction at 1st durability test

(b) Prediction at 2nd durability test

(c) Zoom in prediction at 1st durability test

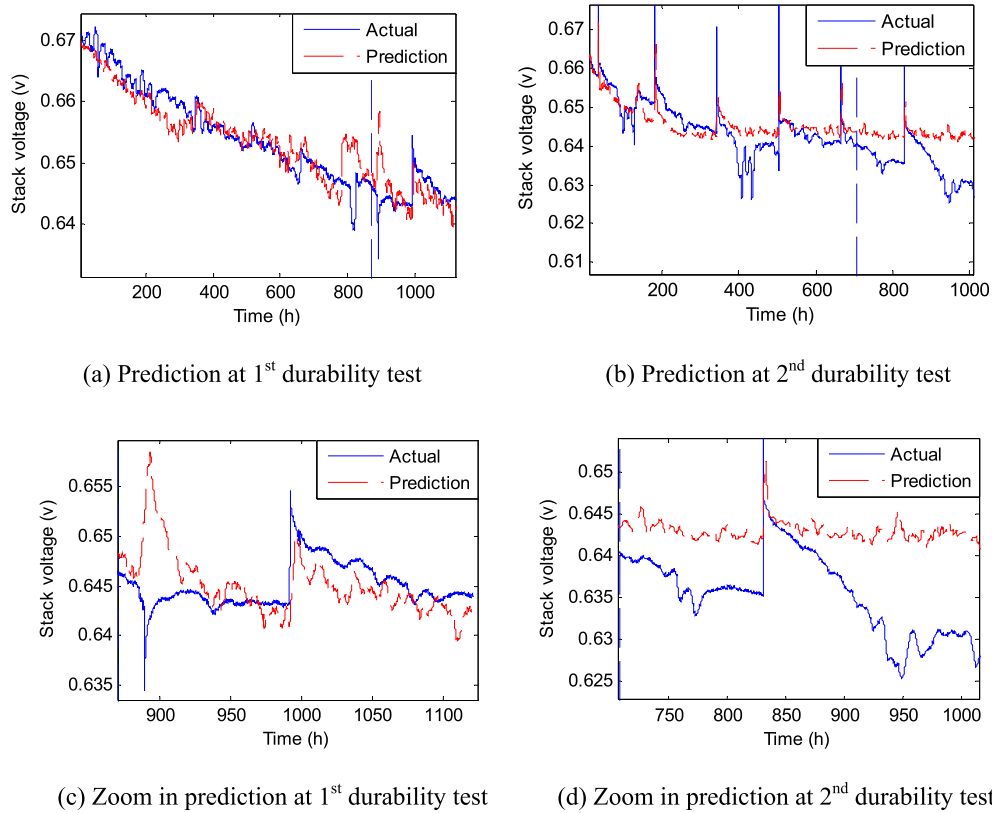(d) Zoom in prediction at 2nd durability test

Fig. 8. Performance of ANFIS in training and predicting fuel cell stack voltage (vertical dashed line separates the training and test data) for two durability tests.

Table 11
Comparison of fuel cell prognostic approaches (where states 1 and 2 represent the steady state and dynamic loading condition, respectively).

Prognostic technique		Computational time (min)	Prediction error (V)
ANFIS	1	1.8	2.71×10^{-4}
	2	2.9	0.04
Particle filtering	1	8.5	0.0053
	2	14.5	0.0068

during its lifetime is investigated using collected polarization curves. For this purpose, a PEM fuel cell behaviour model is used, with its model parameters corresponding to different fuel cell losses. Both fuel cell model parameter variations at steady state and dynamic condition are studied, and results show that ohmic loss provides the dominant contribution for the PEM fuel cell degradation in this study, and model parameters show larger variation at dynamic condition, leading to the shorter lifetime of PEM fuel cell system at dynamic conditions.

With obtained model parameter evolution, particle filtering approach is used to predict the future values of model parameters and thus the PEM fuel cell future performance. From the results, reliable fuel cell performance can be predicted at both steady state and dynamic conditions. Moreover, compared with prognostic results from ANFIS, prediction of model parameters using particle filtering approach can provide better prediction at dynamic conditions, indicating that the proposed method can capture the PEM fuel cell internal behaviour with good quality. From the results, the maintenance strategies can be designed to guarantee the reliable operation of PEM fuel cells, i.e., the fuel cells should be replaced if the predicted voltage/power is below the threshold value, which is defined to indicate the output voltage/power cannot meet the requirements for normal operation.

References

[1] S. Giurgea, R. Tirnovan, D. Hissel, R. Outbib, An analysis of fluidic voltage statistical correlation for a diagnosis of PEM fuel cell flooding, Int. J. Hydrogen Energy 38 (2013) 4689–4696.
[2] N. Fouquet, C. Doulet, C. Nouillant, G.D. Tanguy, B.O. Bouamama, Model based PEM fuel cell state-of-health monitoring via ac impedance measurements, J. Power Sources 159 (2006) 905–913.
[3] M.M. Kamal, D. Yu, Model-based fault detection for proton exchange membrane fuel cell systems, Int. J. Eng. Sci. Technol. 3 (2011) 1–15.
[4] R. Onanena, L. Oukhellou, E.E. Come, S. Jemei, D. Candusso, D. Hissel, P. Aknin, Fuel cell health monitoring using self organizing maps, Chem. Eng. Trans. 33 (2013) 1021–1026.
[5] R. Petrone, Z. Zheng, D. Hissel, M.C. Pera, C. Pianese, M. Sorrentino, M. Becherif, N. Yousfi-Steiner, A review on model-based diagnosis methodologies for

PEMFCs, Int. J. Hydrogen Energy 38 (2013) 7077—7091.

[6] L. Placca, R. Kouta, Fault tree analysis for PEM fuel cell degradation process modelling, Int. J. Hydrogen Energy 36 (2011) 12393—12405.

[7] L.A.M. Riascos, M.G. Simoes, P.E. Miyagi, A Bayesian network fault diagnostic system for proton exchange membrane fuel cells, J. Power Sources 165 (2007) 267—278.

[8] L.A.M. Riascos, M.G. Simoes, P.E. Miyagi, On-line fault diagnostic system for proton-exchange membrane fuel cells, J. Power Sources 175 (2008) 419—429.

[9] Z. Zheng, R. Petrone, M.C. Pera, D. Hissel, M. Becherif, N.Y. Steiner, M. Sorrentino, A review on non-model based diagnosis methodologies for PEM fuel cell stacks and systems, Int. J. Hydrogen Energy 38 (2013) 8914—8926.

[10] B. Legros, P.X. Thivel, Y. Bultel, M. Boinet, R.P. Nogueira, Accoustic emission: towards a real-time diagnosis technique for proton exchange membrane fuel cell operation, J. Power Sources 195 (2010) 8124—8133.

[11] Z. Li, R. Outbib, D. Hissel, S. Giurgea, Data-driven diagnosis of PEM fuel cell: a comparative study, Control Eng. Pract. 28 (2014) 1—12.

[12] L. Mao, L. Jackson, S.J. Dunnett, 'Fault diagnosis of practical polymer electrolyte membrane (PEMF) fuel cell system with data-driven approaches,' Fuel Cells DOI: 10.1002/fuce.201600139.

[13] J. Chen, B. Zhou, Diagnosis of PEM fuel cell stack dynamic behaviours, J. Power Sources 177 (2008) 83—95.

[14] Y. Vural, D.B. Ingham, M. Pourkashanian, Performance prediction of a proton exchange membrane fuel cell using the ANFIS model, Int. J. Hydrogen Energy 34 (2009) 9181—9187.

[15] S. Becker, V. Karri, Predictive models for PEM-electrolyzer performance using adaptive neuro-fuzzy inference systems, Int. J. Hydrogen Energy 35 (2010) 9963—9972.

[16] R.E. Silva, R. Gouriveau, S. Jemei, D. Hissel, L. Boulon, K. Agbossou, N.Y. Steiner, Proton exchange membrane fuel cell degradation prediction based on Adaptive Neuro-Fuzzy Inference Systems, Int. J. Hydrogen Energy 39 (2014) 11128—11144.

[17] L. Mao, L. Jackson, Selection of optimal sensors for predicting performance of polymer electrolyte membrane fuel cell, J. Power Sources 328 (2016) 151—160.

[18] F.N. Buchi, G.G. Scherer, In-situ resistance measurements of Nation 117 membranes in polymer electrolyte membrane fuel cells, J. Electroanal. Chem. 404 (1996) 37—43.

[19] J. Hou, A study on polarization hysteresis in PEM fuel cell by galvanostatic step sweep, Int. J. Hydrogen Energy 36 (2011) 7199—7206.

[20] T.J. Schmidt, Durability and degradation in high-temperature polymer electrolyte fuel cells, ECS Trans. 1 (2006) 19—31.

[21] M. Jouin, R. Gouriveau, D. Hissel, M.C. Pera, N. Zerhouni, Prognostics of PEM fuel cell in a particle filtering framework, Int. J. Hydrogen Energy 39 (2014) 481—494.

[22] M. Jouin, R. Gouriveau, D. Hissel, M.C. Pera, N. Zerhouni, Joint particle filters prognostics for proton exchange membrane fuel cell power prediction at constant current solicitation, IEEE Trans. Reliab. 65 (2016) 336—349.

[23] M. Jouin, R. Gouriveau, D. Hissel, M.C. Pera, N. Zerhouni, Remaining useful life estimates of a PHM fuel cell stack by including characterization induced disturbances in a particle filter model, in: Proc. International Discussion on Hydrogen Energy and Applications, IDHEA Nantes, France, May 2014.

[24] J.T. Pukrushpan, Modeling and Control of Fuel Cell Systems and Fuel Processors, Doctoral dissertation, The University of Michigan, USA, 2003.

[25] T. Selyari, A.A. Ghoreyshi, M. Shakeri, G.D. Najafpour, T. Jafary, Measurement of polarization curve and development of a unique semi-empirical model for description of PEMFC and DMFC performances, Chem. Industry Chem. Eng. Q. 17 (2011) 207—214.

[26] T. Ous, C. Arcoumanis, Degradation aspects of water formation and transport in proton exchange membrane fuel cell: a review, J. Power Sources 240 (2013) 558—582.

[27] C.Y. Chen, H.C. Cha, Strategy to optimize cathode operating conditions to improve the durability of a direct methanol fuel cell, J. Power Sources 200 (2012) 21—28.

[28] D. Verstraete, K. Lehmkuehler, A. Gong, J.R. Harvey, G. Brian, J.L. Palmer, Characterisation of a hybrid, fuel cell based propulsion system for small unmanned aircraft, J. Power Sources 250 (2014) 204—211.

[29] FCLAB research, IEEE PHM Data Chall. (2014), 2014, http://eng.fclab.fr/ieee-phm-2014-data-challenge/.